In-situ monitoring of 2D materials epitaxy during chemical vapor deposition

LayTec's in-situ metrology systems EpiTT and EpiCurve® TT enable close control of key deposition parameters during epitaxial deposition of 2D materials like Graphene, WS_2 or hexagonal boron nitride (hBN). Wafer temperature and surface coverage can be directly deduced thereby accelerating the research on 2D materials and the scale up for industrial production.

Graphene and other sp^2-bonded 2D monolayer materials like hexagonal boron nitride (hBN) and tungsten disulfide (WS_2) are opening up exciting new device and materials possibilities.

Thermal chemical vapor deposition (CVD) is among the most promising methods to synthesize 2D materials that are usually characterized by well-established ex-situ techniques like Raman spectroscopy, atomic force microscopy, etc. after deposition of the respective samples. In contrast, LayTec's EpiTT and EpiCurve® TT metrology systems are able to monitor such processes directly during deposition by means of reflectance and deflection measurements as well as emissivity-corrected pyrometry. They can be integrated into e.g. AIXTRON deposition systems (Fig. 1) and are frequently applied to monitor and control the heteroepitaxy of compound semiconductors on different substrates in applications ranging from optoelectronics (LEDs, lasers) to electronics (HEMT, WBG power electronics).

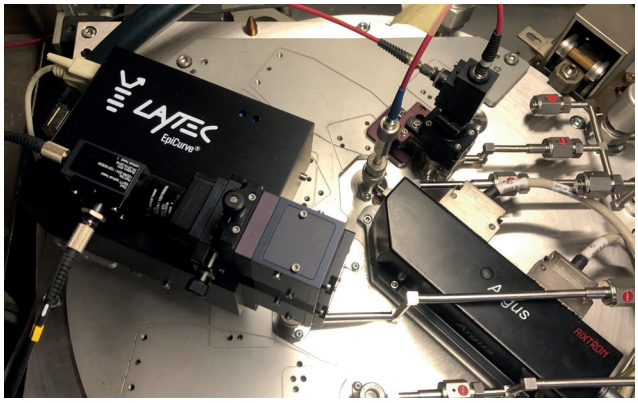

Fig. 1 LayTec EpiCurve® TT mounted on an AIXTRON CCS UVC reactor customized for 2D-material depositions (courtesy of AIXTRON Ltd.)

In this application note, we illustrate some of the results achieved by monitoring CVD deposition processes in an AIXTRON CCS reactor, and show how LayTec metrology systems can help increasing reproducibility and yield in CVD production of 2D materials.

All of the steps involved in a CVD process (precursor dissociation, adsorption, surface diffusion, island nucleation and growth) are thermally activated. Therefore, a reproducible process temperature measurement is of paramount importance for the control and repeatability of the deposition.

Furthermore, reflectance is measured at 950 nm, 633 nm and 405 nm. If the optical contrast between substrate and epi-layer is sufficiently high, reflectance variations can also be measured during the growth of 2D materials with sub-monolayer coverage. In this case, the reflectance measures the surface coverage within the measurement spot, and its variation describes the different growth stages as sketched below. Usually, growth starts with the nucleation of some islands. If their density is too low, the reflectometer may not detect the reflectance variation. Once a critical density of nucleation sites and absorbed atoms is reached, islands grow by bonding diffusing adatoms. The reflectance starts changing with a rate depending on the specific reaction conditions until the growth is stopped or the kinetics of the process change. If the growth is stopped too early, some islands are not coalesced, and the film is discontinuous. If it continues, all islands coalesce, and a continuous film is formed.

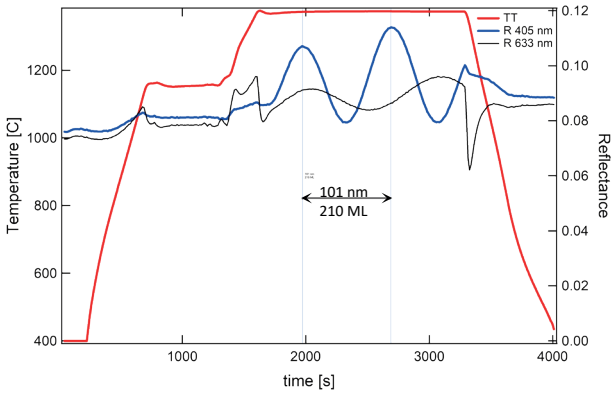

Fig. 2 Temperature and reflectances measured during the deposition of an epitaxial film of hBN on a ssp sapphire wafer. The reflectance oscillation allows to deduce the thickness of the hBN layer from in-situ data.

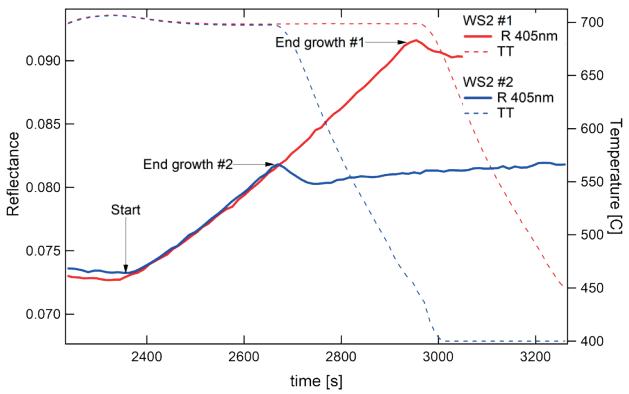

Fig. 3: Temperature and reflectances measured during the deposition of an epitaxial film of WS_2 on a ssp sapphire wafer. The reflectance values allow to deduce the surface coverage Θ with WS_2.

For a self-limiting process both, growth and reflectance variation rate, will slow when approaching the full monolayer in phase. But, if no barrier prevents or slows down the growth after the completion of the first monolayer, the reflectance will change steadily until the process is stopped or the material-specific bulk reflectance value for the deposited material is reached.

hBN on sapphire

Fig. 2 shows the results measured during the epitaxial deposition of hBN on sapphire. The carrier temperature is accurately measured throughout the deposition run. 2D material films are usually very thin, and shorter wavelengths are more sensitive for their characterization. This is illustrated by the reflectance comparison at 405 nm and 633 nm: the 405 nm trace shows two fully developed oscillations, with a higher amplitude than the 633 nm trace and is better suited for deducing the hBN layer thickness. Here a quite thick layer (ca. 260 nm or 475 ML) of hBN was deposited. The interference between light reflected at the buried interface and at the gas-solid interface determines the reflectance oscillatory pattern: accurate knowledge of the optical constants at the process temperature will allow precise in-situ measurement of the material thickness during the deposition itself.

WS_2 on sapphire

Fig.3 illustrates the growth of WS_2 for different coverages (Θ = 0.5, Θ = 1, stacked monolayers).

WS_2 deposition took place at 700°C. The growth runs WS2_#1 and WS2_#2 were performed under the same conditions of temperature, pressure and precursors flows but different deposition times (t_d): t_d(WS2_#1) = 2t_d(WS2_#2). AFM investigations confirmed that the coverage Θ is proportional to the growth duration: Θ(WS2_#2) = 0.5 and Θ(WS2_#1) = 1.

The reflectance variation (ΔR) at 405 nm between sapphire with Θ = 0 and Θ = 1 ML WS_2 is 1.9% in good agreement with the expected value of 2.0% (based on [2]). ΔR is proportional to the deposition time t_d in the interval between t_{start} and t_{end}, indicating that ΔR is a measure of the surface coverage with WS_2.

Looking at the initial stage of the deposition, Fig. 3 shows that the growth starts directly when the precursor is introduced into the chamber without an induction period for island nucleation.

Since R_{405} is proportional to Θ(WS_2), a change in R_{405} slope would indicate a change in the reaction kinetics.

Fig. 4 shows reflectance traces for three different growth runs resulting in layers of different thicknesses: sub-monolayer, monolayer, stacked layers. The growth conditions for the runs “Submonolayer” and “Stacked” are the same but their duration is different. Since R_{405} slope does not change with the transition from single monolayer to stacked monolayers, we conclude that the nucleation of the 2nd layers is not hindered by a kinetic barrier.

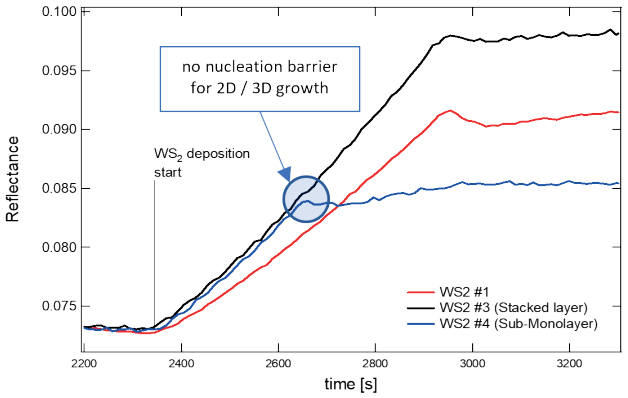

Fig. 4: Results of deposition of WS2 layers of different thickness: sub-monolayer, monolayer, stacked layers. The growth conditions for the runs "Submonolayer" and "Stacked" are the same for different durations.

Graphene on sapphire

This section focusses on graphene CVD on single side polished (ssp) sapphire. The graphene has been deposited at 1420°C, using methane as a precursor, in a direct van der Waals epitaxy process. Under these conditions, the precursor molecules dissociate completely in the gas phase. In a simplified view of the process, the carbon atoms get adsorbed and diffuse on the surface until they either desorb (thermally or after reaction with O from the sapphire) or coalesce with other C atoms to start nucleation islands. If they overcome a critical size, these islands continue to grow and may eventually coalesce into a film (see [3] and references therein for a more detailed description of this process).

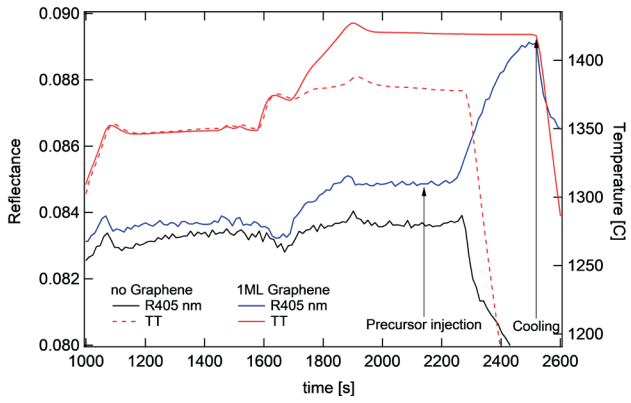

Fig. 5: Data collected during two similar runs: "no Graphene" – the sapphire was heated to 1347°C and 1370°C, but no precursor was injected into the chamber; "1 ML Graphene" – the sapphire substrate was heated up to 1347°C and then to 1420°C. The wafer has been exposed to the precursor for 380s, at 1420°C. Then the precursor flow was stopped, and the reactor was cooled down.

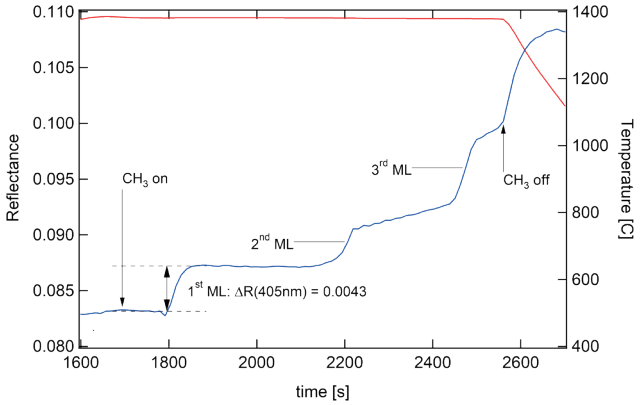

Fig. 6: Evolution of R_{405} with graphene coverage Θ between Θ=0 and Θ=3. The island nucleation starts when the precursor is introduced into the chamber, but the reflectance starts to be affected only after ca. 80 s allows for the deposition, possibly when the islands start expanding. Upon island coalesce, the full coverage of the surface with the 1st ML of graphene is completed and the further increase of the reflectance is stopped. Increasing the partial pressure of the precursor allows the deposition of further monolayers.

Fig. 5 shows the data collected during two runs. In one of them ("no Graphene") the substrate only underwent the thermal cycle with temperature steps at 1347°C and 1370°C, but no precursor was injected into the chamber. In the run "1 ML Graphene", the sapphire substrate was heated up to 1347°C and then to 1420°C, when the deposition of 1 ML graphene took place by allowing the precursor for 380s in the chamber. After that the precursor flow was stopped, and the reactor was cooled down. Ex-situ Raman spectroscopy measurements confirmed the presence of 1-2 ML of graphene. The 405 nm reflectance tends toward a maximum suggesting the existence of an energetic barrier for the nucleation of further monolayers.

In Fig. 6 we illustrate in detail the deposition of up to 3 ML graphene. As mentioned earlier, the reflectance at 405 nm (R_{405}) remains constant after saturation of the first monolayer: its variation is $\Delta R(\Theta=1)405 = 0.0043$. Between 1900s and 2100s, despite the availability of the precursor, the reflectance remains constant because an energetic barrier prevents the nucleation of further monolayers. Carefully adjusting the process conditions allow for the controlled deposition of the second and third monolayers: this process is mirrored by the increase in R_{405}.

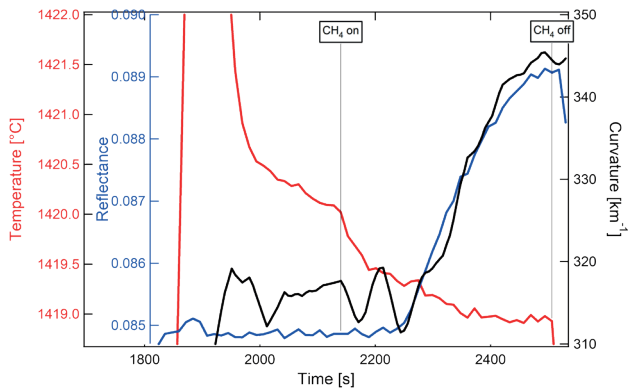

Fig. 7: Comparison of the changes in reflectance and curvature signal during CVD of graphene. It can be seen that the change in curvature closely follows the change of the reflectance signal at 405 nm.

The comparison with the growth of WS_2 (Fig. 4) shows some remarkable differences:

– Graphene growth shows the existence of an induction period for the onset of 1st ML nucleation, different from the instantaneous growth in the case of WS_2.

– Investigating the R_{405} allows to monitor the completion of the first MLs. The stepwise increase of R_{405} indicates the existence of a barrier to the nucleation of each ML. This is different from the growth of WS_2 (Fig. 4), where the reflectance variation showed no changes in the transition between 1st ML and 2nd ML.

– Monitoring R_{405} enables process control for industrial applications.

Ex-situ Raman spectroscopy measurements confirmed the presence of 3 ML of graphene.

Fig. 7 illustrates the substrate curvature changes upon deposition of a single graphene monolayer as measured by LayTec's EpiCurve TT. The driving force for this deformation is the vertical thermal gradient through the wafer heated in the reactor [4]: the wafer bottom (in contact with the hot susceptor) is hotter than the wafer top (cooled by the process gas). So, sapphire thermal expansion is more pronounced close to the substrate than at the interface with the gas, and the wafer assumes a concave shape. Moreover, the increase in surface emissivity upon graphene deposition further reduces the surface temperature, enhancing the vertical thermal gradient through the wafer and its concave curvature.

Conclusions

It has been shown how LayTec's EpiTT and EpiCurve® TT allow for in-situ monitoring of 2D materials deposition and thereby offer new means to control these complex processes in-situ right during deposition. A precise measure of wafer temperature ensures tighter process control. Moreover, measuring the variation of the surface reflectance during the growth reveals details on the deposition kinetics and enables an accurate control of the number of deposited monolayers already during the process.

Acknowledgments

We thank:

– AIXTRON Ltd. for granting the machine time to perform the growth and for ex-situ characterization as well as for the valuable discussion.

– German Federal Ministry of Education and Research (BMBF) for partial funding the project GIMMIK – Graphene Processing on 200 mm wafers for microelectronic applications (Grant 03XP0210F).

References:

[1] https://www.laytec.de/epitt

[2] Yilei Li et al., PHYSICAL REVIEW B 90 (2014) 205422

[3] J. Hwang et al., ACSNANO, 7(1) (2013) 385

[4] F. Brunner et al., J. Crystal Growth 289 (2007) 202

LayTec AG
Seesener Str. 10-13
10709 Berlin, Germany

Tel.: +49 (0)30 89 00 55-0
Email: info@laytec.de
Web: laytec.de